FRICTION STIR WELDING AT MSFC: KINEMATICS

Arthur C. Nunes, Jr.
Marshall Space Flight Center
ED33, Huntsville, AL 35812
(256) 544-2699
arthur.nunes@msfc.nasa.gov

Introduction. In 1991 The Welding Institute of the United Kingdom patented the Friction Stir Welding (FSW) process (Thomas *et al*.). In FSW a rotating pin-tool is inserted into a weld seam and literally stirs the faying surfaces together as it moves up the seam. By April 2000 the American Welding Society International Welding and Fabricating Exposition featured several exhibits of commercial FSW processes and the 81st Annual Convention devoted a technical session to the process.

The FSW process is of interest to Marshall Space Flight Center (MSFC) as a means of avoiding hot-cracking problems presented by the 2195 aluminum-lithium alloy, which is the primary constituent of the Lightweight Space Shuttle External Tank. The process has been under development at MSFC for External Tank applications since the early 1990's.

Early development of the FSW process proceeded by cut-and-try empirical methods. A substantial and complex body of data resulted. A theoretical model was wanted to deal with the complexity and reduce the data to concepts serviceable for process diagnostics, optimization, parameter selection etc.

A first step in understanding the FSW process is to determine the kinematics, i.e. the flow field, in the metal in the vicinity of the pin-tool. Given the kinematics, the dynamics, i.e. the forces, can be targeted. Given a completed model of the FSW process, attempts at rational design of tools and selection of process parameters can be made.

The dynamic anomaly. The attempts to model the FSW process at MSFC began with a cylindrical rotating flow matching the surface speed of the rotating pin-tool at the pin surface and extending out to some radius at which the flow stops. The heat generated would leak out radially into the workpiece, and the mechanical work would balance the heat loss. At steady state the moments on a ring element cut out of the swirl would balance to zero. A simple system of equations could be written to model the distribution of angular velocity throughout the deformation zone.

The stress on the outside of a ring element has the advantage over that on the inner surface. The area is bigger; the moment arm is longer. For equilibrium, then, the flow stress has to decrease with increasing radius. For metals the flow stress is not greatly affected by shearing rate, but mainly by temperature. Hence, the temperature must increase with radius. The heat generated from the plastic flow has to flow backwards down the temperature gradient into the tool! But what if the tool were insulated? With an insulated tool, backflow of heat and the required temperature rise with radius could not occur. This consequence of the plasticity of the workpiece seemed peculiar. It was dubbed a "dynamic anomaly." It led to a reevaluation of assumptions. There are several ways to alter the original assumptions to circumvent the "dynamic anomaly".

Alteration of the constitutive equation of the metal to make the metal viscous would reduce stresses at greater radii by reducing the strain rate so as to make it unnecessary for the temperature to drop. This approach was rejected because no good justification for attributing viscous behavior to a metal could be found. See Appendix 2.

Withdrawal of the assumption of steady-state flow in favor of an oscillatory flow might allow a plausible solution. Stick-slip flow is well known in friction situations. This approach was rejected because oscillations were not observed in FSW flow.

Withdrawal of the assumption of a radially distributed shear in favor of a slip discontinuity, a slip envelope, would also allow a plausible solution. Slip discontinuities are characteristic of plastic flows. This approach was adopted.

The rotating plug model. The rotating plug model superposes two flows: (1) rapid shear over an approximately discontinuous cylindrical boundary separating a plug of metal rotating with the tool from the stationary workpiece metal, and (2) a relatively slow rotating motion driven by the threads on the tool and wrapped around the tool in a ring vortex configuration. See Figure 1.

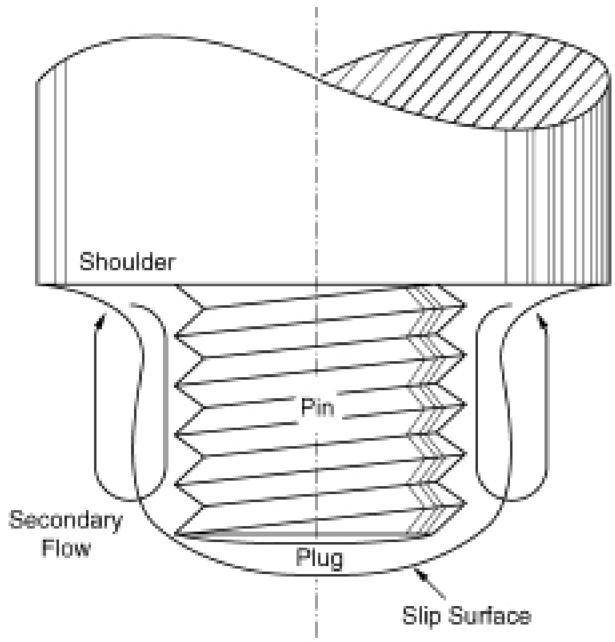

Figure 1. The rotating plug model comprises: (1) a rapidly rotating plug of metal attached to the pin-tool and slipping with respect to the workpiece on a cylindrical surface surrounding the pin-tool, and (2) a relatively slow circulation driven by the threads surrounding the pin as a vortex ring.

As the tool moves it is necessary for metal to pass from the front to the back of the tool. One way for this to occur is by a wiping motion. A wiping motion can be modeled by superposing a rotating disc velocity field

$$\vec{V} = -y\Omega\vec{i} + x\Omega\vec{j} \tag{1}$$

upon the velocity field of a uniform displacement

$$\vec{V} = -V\vec{i} \tag{2}$$

It is noted in passing that if volume is conserved ($\nabla \cdot \vec{V} = 0$) in each of the fields, it is conserved in their superposition. The velocities of the superposition field on the disc are

$$\frac{dx}{dt} = -(y\Omega + V) \tag{3}$$

and

$$\frac{dy}{dt} = x\Omega \tag{4}$$

The trajectory on the disc is computed by equating expressions for dt in the above equations.

$$xdx + \left(y + \frac{V}{\Omega}\right)d\left(y + \frac{V}{\Omega}\right) = 0 \tag{5}$$

or

$$x^2 + \left(y + \frac{V}{\Omega}\right)^2 = \text{Constant} \tag{6}$$

The resultant trajectories are circles displaced towards the forward moving side of the rotating disc (or the $\vec{V} x \vec{\Omega}$ direction). The resultant flow field is shown in Figure 2. For FSW normally $\frac{V}{\Omega} << r$, where r is the radius of the rotating plug. Hence the metal flow takes place in a thin layer on the surface of the rotating plug. Figure 2 greatly exaggerates the width of the wiping deformation layer just under the surface of the rotating plug.

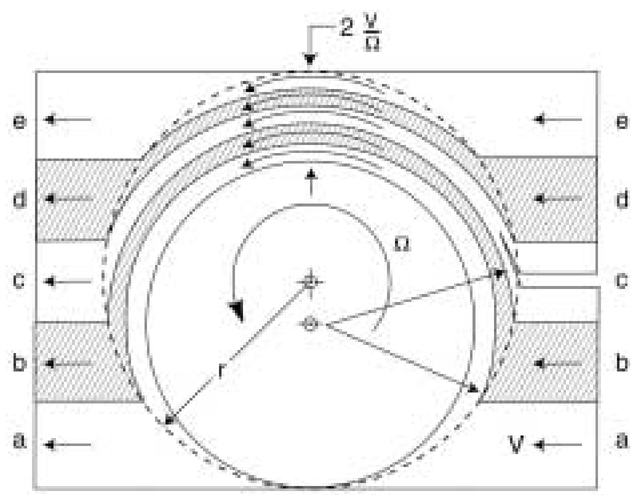

Figure 2. Wiping flow is modeled by superposing a rotating disc on a uniform translation. Trajectories on the disc are circles with radius displaced by $\frac{V}{\Omega}$ towards the advancing side of the disc. When $r\Omega >> V$, as is generally the case for FSW, flow about the central plug takes place in a thin layer ranging from zero to $2\frac{V}{\Omega}$ in thickness. Note that in this model metal exits the disc at the same position that it enters.

Because it is easy to visualize this model using people walking across a merry-go-round, it is sometimes referred to as the "merry-go-round" model. Imagine a person walking towards and stepping onto a merry-go-round. If the person continues to walk in the same direction (not an easy feat on a real merry-go-round), he moves into the rotating disc until he passes the disc center, then he moves out to the edge again in a symmetric trajectory. Because of the symmetry, he gets off at the same distance from the centerline as he gets on. That is, the rotation does not shift his ultimate y-position.

Tracer Experiments. Tracer experiments (See Figure 3) have been carried out at the University of South Carolina (Reynolds *et al*) where a FS weld is passed through a band of tracer metal of different, distinguishable composition.

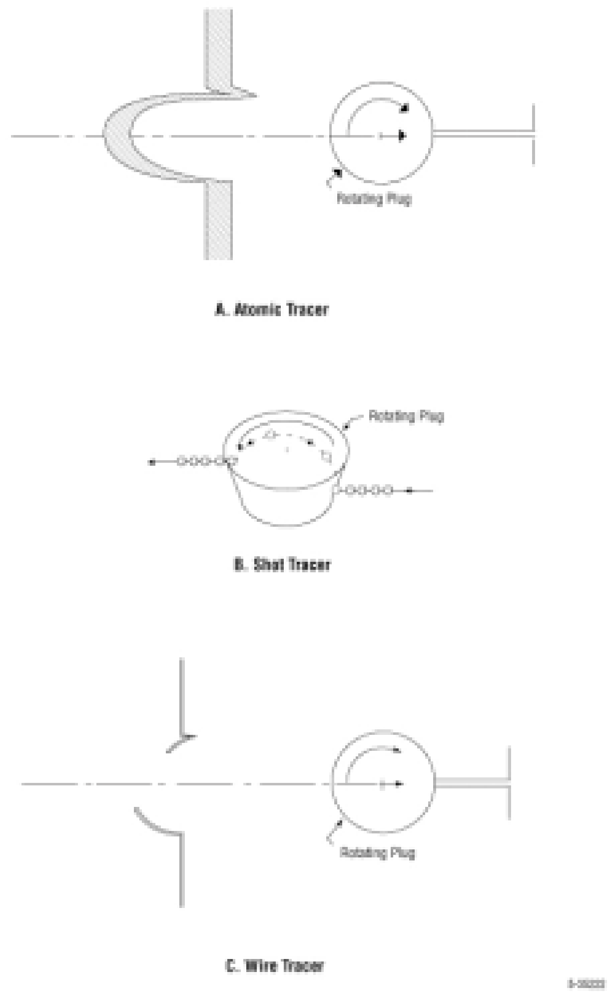

Figure 3. FSW tracer experiments.

A trailing parabolic loop of tracer metal is left behind the tool. The observed dimensions of the loop seem to agree with the rotating plug concept in that the particles appear to be displaced back from the original band by approximately the chord of the plug circle. Further, there is a forward pointing spur of tracer ahead of the original band on the forward moving side of the plug as if material being carried around the plug surface dropped off before

completing the circuit around the plug. The premature exiting of material from the rotating plug can be attributed to the secondary vortex flow.

Steel shot tracer experiments carried out at Boeing Company's Seattle, Washington, plant (Colligan) reveal a complex behavior that can be interpreted in terms of (1) the basic wiping flow characterized in Figure 2, (2) the variation in plug diameter with depth, and (3) a shifting of material with respect to the plug by the secondary flow.

For example, shot entrained by the rotating plug is not left behind at the same distance from the centerline as it entered. This is because the vortex circulation shifts the shot into an axial site where the plug radius is different. If the plug radius variation is large with respect to axial displacement along the pin close to the tool shoulder, the lateral displacement of the shot becomes more sensitive to slight variations in axial displacement. This is taken to be the reason why the shot patterns exhibit a great deal of scatter in the proximity of the tool shoulder.

At Marshall Space Flight Center the effect of the FSW tool on wire tracers (Bernstein *et al.*) was found to support the concept of the rotating plug model. Copper wires were inserted into holes drilled perpendicular to the weld interface at different plate depth levels. The wires on the forward moving side of the pin-tool were bent forward and broken. The wires on the retreating side of the pin-tool were swept backwards into a trailing curve. The shapes of the trailing curves were computed for different distributions of angular velocity around the pin-tool. The computations that agreed best with the observations were those for the sharpest drop-off of the angular velocity, i.e. the computations closest to the sharp discontinuity of the rotating plug model.

Strain Rates. The idealized wiping model presented here does not yield a strain rate. Each stream of metal approaching the rotating plug at a different lateral position receives its own instantaneous shear increment as it crosses the shear interface. The sheared metal has a certain time at the temperature of the shear zone for recovery. Then the metal receives a second shear increment as it exits from the rotating plug.

It is possible to estimate a representative shear rate, however. The metal flows into the plug of radius r over a path of width 2r. By the time it has been swept to the side of the plug, $\frac{\pi}{2\Omega}$, the stream of metal is narrowed to $2\frac{V}{\Omega}$ for a tensile strain of $\frac{r\Omega}{V}$. The strain rate $\dot{\varepsilon}$ is approximately

$$\dot{\varepsilon} \sim \frac{2}{\pi}\frac{r\Omega^2}{V} \tag{7}$$

If r = 0.22 inches, V = 5.25 inches/minute, and $\Omega = 2\pi(350\text{ RPM})$, then the resulting strain rate is 2150 $\sec^{-1}$. This is high, in the range of metal cutting strain rates.

This strain rate estimate, more of a lower bound, perhaps, than a mean, is of interest in that it appears to have a potential for estimating the microstructure of a FS weld.

One approach is to approximate the link between mechanical strain and resulting microstructure by a dynamic recovery process. These softening processes all involve "single dislocations, which are annihilated in individual events" (McQueen and Jonas p. 438). A correlation has been published (McQueen and Jonas p. 409) between the subgrain diameter d of commercial purity aluminum and the Zener-Holloman parameter (Zener and Holloman), $Z \equiv \dot{\varepsilon}e^{\frac{37,300}{RT}}$ $\sec^{-1}$, where $\dot{\varepsilon}$ is the applied strain rate, R, the Gas Constant, and T the absolute temperature during deformation:

$$d = \frac{1}{0.08\log Z - 0.6} \tag{8}$$

The approximate correlation holds for Z's less than 10^{18}. The highest strain rate listed in the experimental data is 219 sec^{-1}.

An attempt (Frigaard *et al*) was made to use this relation to work backwards from measured subgrain diameters and estimate the strain rates in FS welds in AA6082 and AA7108 aluminum extrusions (conforming to 6082-T6 and 7108-T79 alloys). Rates obtained in this way were extremely low, 1 to 20 sec^{-1}. Frigaard *et al* attribute the discrepancy between their low strain rate estimates and the much higher strain rates expected from the nature of the mechanical process to melting "a liquid film at the tool/matrix interface".

An explanation more in consonance with the concept of the FSW process expressed herein would be that at the high strain rates dynamic recrystallization, "where dislocations are annihilated in large numbers through the migration of a high angle boundary" (McQueen and Jonas p.438), accounts for much of the structural transformation during mechanical deformation.

In any case a means for linking the mechanically estimated strains with the FSW microstructure does not exist at present. The understanding of the transformations that annihilate dislocations at high strain rates is not adequate.

Conclusions. The rotating plug model of the FSW process explains complex-seeming results of tracer experiments well and simply. It is thought to be fairly well substantiated.

The model permits a rudimentary estimate of the FSW strain rate. An estimation of the FSW microstructure from the strain rate, however, awaits a better understanding of recovery and recrystallization dynamics at high strain rates.

Even in its present state of development, the model is a potentially useful tool in fault diagnostics, and a correct kinematics is a prerequisite for constructing a dynamics (Nunes *et al*) of the FSW process.

References.

Backofen, Walter A. 1972. Deformation Processing. Addison-Wesley Publishing Company: Reading, MA.

Bernstein, E.L. and Nunes, A.C., Jr. 2000. The Plastic Flow Field in the Vicinity of the Pin-Tool during Friction Stir Welding. Under review by *Welding Journal*.

Colligan, K. 1999. Material Flow Behavior during Friction Stir Welding of Aluminum. *Welding Journal* 78(7): 229-s to 237-s.

Crandall, Steven H. 1956. *Engineering Analysis: A Survey of numerical procedures*. McGraw-Hill Book Company, Inc.: New York.

Frigaard, Ø., Grong, Ø., Hjelen, J., Dulbrandsen-Dahl, S. and Midling, O.T. 1999. Characterization of the subgrain structure in friction stir welded aluminium alloys using the SEM-EBSD technique. *1st International Symposium on Friction Stir Welding*, Rockwell Science Center, Thousand Oaks, CA. June 14-16.

Hill, R. 1950. *The Mathematical Theory of Plasticity*. Oxford at the Clarendon Press: New York.

McQueen, H.J. and Jonas, J.J. 1975. Recovery and Recrystallization during High Temperature Deformation. *Treatise on Materials Science and Technology, Volume 6: Plastic Deformation of Metals*, R.J. Arsenault, Ed. Academic Press: New York. 393-493.

Nunes, A.C., Jr., Bernstein, E.L. and McClure, J.C. 2000. A Rotating Plug Model for Friction Stir Welding. 81st AWS Annual Convention, Chicago, IL, April 25-28.

Reynolds, A.P., Seidel, T.U., and Simonsen, M. 1999. Visualization of Material Flow in an Autogenous Friction Stir Weld. *1st International Symposium on Friction Stir Welding*, Rockwell Science Center, Thousand Oaks, CA. June 14-16.

Thomas, W.M., *et al.*. Dec. 1991. Friction Stir Welding. U.S. Patent 5,460,317.

Zener, C. and Holloman, J.H. 1944. Effect of Strain Rate Upon Plastic Flow of Steel. *Journal of Applied Physics*. 15, January.22-32.

APPENDIX 1

Nomenclature

d	Subgrain diameter
$\vec{i}, \vec{j}$	Unit vectors in x- and y-directions respectively
t	Time
$\vec{V}$	Translational velocity of pin-tool
V	Weld speed
x	Distance from center of rotating pin in direction of movement
y	Distance from center of rotating pin perpendicular to linear movement in direction of retreating side of pin
$\dot{\varepsilon}$	Strain rate
$\vec{\Omega}$	Angular velocity of pin
Ω	Magnitude of angular velocity of pin

APPENDIX 2

Viscous theories of the FSW flow field. It is tempting to try to construct a viscous model of the FSW flow field. A viscous flow field will be continuous and distributed as initially expected. But the assumption of viscosity requires physical justification. As the apparent operating temperatures are substantially below the alloy solidus temperature, justification of the assumption of viscosity presented greater difficulties than abandonment of the expectation of a continuous, distributed FSW flow field.

Metals have flow characteristics unlike those of gases or liquids. When a layer of gas is sheared, gas molecules with speeds matched to the moving boundaries by collisions with the boundaries transfer momentum by intermolecular collisions through the layers of gas between the boundaries. The momentum transfer results in a viscous shear force on the boundaries. A rise in temperature promotes more momentum transfer so that the viscosity of gases goes up with increasing temperature.

When a layer of liquid is sheared random local structural rearrangements ease the shear force transmitted by the elastic character of the liquid. In doing so they determine the level of stress across the liquid layer. These local structural rearrangements come into play at the lowest of stress levels and in whatever direction the stress is acting. Thus liquids exhibit viscous behavior. The viscosity of liquids, unlike that of gases, goes down with increasing temperature, however, because thermal energy aids local structural rearrangements of liquids.

When a layer of metal is sheared, the metal at first deforms elastically. Only after a sufficiently high stress is imposed do the internal dislocation sources begin to emit so that plastic flow occurs. If structural changes leading to work hardening are ignored, the flow stress of a metal remains constant. Metals are not viscous. They are plastic. That is, the stress is whatever is applied up to the flow stress, but a stress higher than the flow stress cannot be applied; the metal merely flows at this point.

Because the flow stress of metals is only weakly dependent upon strain rate, the metallic stress-strain curve is more or less independent of strain rate, which is not at all the case for viscous materials. A simple dislocation mechanism of metallic flow yields a dependence of flow stress on the logarithm of the strain rate. Although metals are not viscous, the dislocation emission process is thermally activated so that the flow stress of metals depends strongly upon temperature.

This is why plasticity theory (Hill, Backofen), which amounts to the solution of a hyperbolic system of equations (Crandall), where characteristic lines exist along which there can be discontinuities, is so different from a (incompressible) viscous flow theory, which employs parabolic or elliptical systems of equations.